The Astrophysical Journal, 579:905–913, 2002 November 10

SATURN TROJANS: STABILITY REGIONS IN THE PHASE SPACE

F. Marzari and P. Tricarico
Dipartimento di Fisica, University of Padova, Via Marzolo, Padua, Italy;
marzari@pd.infn.it, tricaric@pd.infn.it

and

H. Scholl
Observatoire de la Cote d'Azur, BP 4229, Boulevard de L'Observatory, Nice, Cedex 4 F-06304, France; scholl@obs-nice.fr
Received 2002 April 19; accepted 2002 July 15

ABSTRACT

We use the frequency map analysis method to identify for Trojan orbits of Saturn the regions in the proper orbital element phase space characterized by higher stability. We find that Trojan orbits with proper eccentricity around 0.05, libration amplitude of about 80°, and inclination lower than 15° show a slow diffusion in the proper frequency of the longitude of perihelion $\tilde{\omega}$, which indicates long-term stability. Numerical integration of some of these stable orbits indicates a half-life of about 2.5 Gyr. Orbits with inclination of about 20° are destabilized by a secular resonance with the forcing term $2g_6 - g_5$. At higher inclinations Saturn Trojan orbits are unstable on a short timescale (a few $\times 10^5$ yr). Applying the frequency map analysis to the numbered Jupiter Trojans, we find that the size of the stability region is much larger for Jupiter Trojans than for Saturn Trojans. Moreover, the diffusion rate is significantly lower, suggesting that the dynamical lifetimes of Jupiter Trojans are considerably longer. The frequency analysis method allows us to separate the proper and forced components of the eccentricity of Trojans. A semianalytical model for secular motion of Saturn Trojans is presented.

Subject headings: minor planets, asteroids — solar system: general

1. INTRODUCTION

Jupiter and Saturn are believed to have formed in the same way, by accretion of an icy rocky core followed by the massive infall of nebular gas (Pollack et al. 1996), because both planets appear to have a similar internal structure. During the growth of the two planets, Trojans might have been captured from a reservoir of planetesimals near the planet's orbit by different mechanisms (Marzari et al. 2002). In particular, the rapid mass growth of the giant planets by gas infall is a very efficient mechanism to trap planetesimals into stable Trojan orbits, as shown by Marzari & Scholl (1998a, 1998b). In the case of Jupiter this trapping mechanism has lead to the formation of a large population of Trojans comparable in number to the main belt asteroids (Jewitt, Trujillo, & Luu 2000). Hence, Saturn also could have trapped Trojans like Jupiter. However, no Saturn Trojans have been observed until now. Of course, the detection of Saturn Trojans requires larger telescopes than in the case of Jupiter Trojans since Saturn Trojans are almost a factor of 2 farther away than Jupiter Trojans. On the other hand, the observation of a 100 km sized Saturn Trojan with a magnitude in the range 18–19 mag is not a real problem for 3 m class telescopes. If the Saturn Trojan population were as numerous as the Jupiter Trojan population, at least one Saturn Trojan should have been discovered.

Dynamical instability could simply be the reason for the apparent absence of Saturn Trojans. Another reason might be that there were only very few planetesimals in the reservoir region around Saturn. The migration of Saturn (Gomes 1998) could be another reason as well.

Previous studies on the stability of Saturn Trojans have shown that the stable regions near the Lagrangian points L4 and L5 of Saturn are very small compared to the Jupiter Trojan region. Two basic mechanisms have been identified by different authors for the instability: perturbations due to the near 2 : 5 mean motion resonance between Jupiter and Saturn known as the Great Inequality (de la Barre, Kaula, & Varadi 1996; Innanen & Mikkola 1989; Nesvorný & Dones 2002) and the mixed secular resonance $2g_6 - g_5$ (Marzari & Scholl 2000). Both mechanisms may work separately or combined. The orbit of a Saturn Trojan usually becomes unstable because its eccentricity is increased due to the two mechanisms above until the Trojan has a close encounter with Saturn. Are there dynamically stable regions over the age of the solar system? Nesvorný & Dones (2002) have shown that Saturn's co-orbital region is chaotic in the frame of the planar model keeping Jupiter and Saturn on fixed circular orbits (bicircular model). Chaos is attributed to the overlap of Jupiter's 2 : 5 (Great Inequality) and Saturn's 1 : 1 mean motion resonances. This result indicates that the Saturn Trojan region is intrinsically unstable because of chaos. Computing the maximum Lyapunov characteristic exponents (LCEs) in a nonzero inclination model including the four outer planets, Nesvorný & Dones show that tadpole trajectories near L4 are strongly unstable. There is only a very small region restricted to small eccentricities and inclinations where orbits may survive over timescales of the age of the solar system. Only two of 211 initial Saturn Trojans survived over timescales of 4 Gyr. This result is in agreement with our numerical integrations (Marzari & Scholl 2000).

Before the work of Nesvorný & Dones (2002), Melita & Brunini (2001) had already located dynamical niches of stability possibly over timescales of the age of the solar system by applying basically the Laskar, Froeschlé, & Celetti (1992) and Laskar (1993a, 1993b) frequency map analysis (FMA) method. The advantage of this method

consists in the comparatively short time span for integration required to determine the stability of orbits. This allows a rich statistical sampling of the phase space without an excessive computational effort. Melita & Brunini (2001) give the initial values of the stable orbits in particular coordinates that are not obvious to convert in proper orbital elements. Hence, it is difficult to determine the size of the stable regions.

In this paper, we apply the FMA method, unlike Melita & Brunini (2001), in the phase space of proper orbital elements. This allows a direct comparison with numerical integrations and an interpretation of numerical experiments.

We implemented the FMA method following Laskar et al. (1992), Laskar (1993a, 1993b), and Nesvorný & Ferraz-Mello (1997), and we applied it to a large sample of initial conditions for Saturn Trojans. We have identified where Saturn Trojan orbits are more stable in the proper eccentricity versus proper libration amplitude space. Stability areas are located at low proper eccentricity and large libration amplitudes on orbits that in most cases have the perihelion librating around that of the planet in a condition known as "paradoxical libration" (Beaugé & Roig 2001). We also divide the phase space in to slices with fixed inclination, and we find that there is a progressive shrinking of the stability areas for increasing inclination. At values of inclination $i \geq 20^\circ$ there are no stable orbits.

2. NUMERICAL ALGORITHMS

We have applied the FMA method (Laskar et al. 1992; Laskar 1993a, 1993b) to the outcome of a numerical integration of a total of 5000 Saturn Trojan orbits near both Lagrangian points L4 and L5 of Saturn.

2.1. *The Numerical Integration of Trojan Orbits*

We numerically integrated the orbits of virtual Trojans and the four outer planets Jupiter, Saturn, Uranus, and Neptune with the WHM integrator (Wisdom & Holman 1991; Levison & Duncan 1994) with a fixed step size of 10 days. The code is part of the SWIFT software package that can be downloaded from the ftp site of H. Levison.[1] The starting orbital elements of the planets and Trojans were computed with respect to the invariable plane of the solar system.

The initial orbital elements of the Trojans, except inclinations, were chosen at random with a uniform distribution. Five sets of 1000 orbits with inclinations of 0°, 5°, 10°, 15°, and 20° were integrated. The starting semimajor axes of the Trojans were selected in an interval ranging from $0.99a_S$ to $1.01a_S$, with a_S the semimajor axis of Saturn. The eccentricities were taken between 0 and 0.15. All angle variables were chosen between 0° and 360°. This procedure to select starting values yields a large number of orbits that are rapidly destabilized by planetary perturbations. A body was retained in each final sample of 1000 orbits per fixed inclination only if it survived as a Trojan over 10^5 yr. We noticed in preliminary numerical tests that instability built up either very quickly within 10^5 yr or over a much longer period at least for inclinations up to 20°. All the of five sets of 1000 bodies were integrated over 5 Myr. This integration period is motivated by the FMA method as outlined in the following subsections. Two additional sets of 1000 orbits were generated with $i = 30^\circ$ and $i = 40^\circ$. However, all the bodies in these two samples became unstable on a timescale of a few $\times 10^5$ yr, and hence, they were not analyzed with the FMA method.

We stored at evenly spaced intervals in time for each body the six orbital elements and the critical argument $\lambda_T - \lambda_S$ of the Trojan orbit, where λ_T and λ_S are the mean longitudes of the Trojan and Saturn, respectively. It is well known that the sampling rate has to be chosen carefully in order to avoid aliasing that may lead to misleading results, in particular when we look at the frequencies of the angular variables. For this reason, we applied directly during the integration a low-pass finite impulse response digital filter (Carpino, Milani, & Nobili 1987), and this allowed a correct decimation of the output. The filter removed all the frequencies with period lower than about 100 yr attenuating the short-period terms related to the orbital period of Jupiter, Saturn, and Uranus. Neptune's short periodic perturbations are negligible because of its large distance. The filtered orbital elements were sampled every 273 yr, which generated a final output file of only 1.6 GB.

2.2. *The FMA Method*

The FMA technique was introduced by Laskar et al. (1992) and Laskar (1993a, 1993b), and it is based on the analysis of the evolution with time of the fundamental frequencies that appear in the spectrum of a test of body orbital elements. The amount of diffusion of the frequencies gives a measure for the stability of an orbit.

We recall briefly the FMA theory and the numerical algorithm we have implemented to evaluate the frequencies and their variations. Given a quasiperiodic function $f(t)$, we can represent it in the following form:

$$f(t) = \sum_{k=1}^{\infty} a_k e^{i(\nu_k t + \phi_k)} , \tag{1}$$

where a_k are real amplitudes decreasing with k and ν_k and ϕ_k are the corresponding frequencies and phases, respectively. The basic idea of the FMA is to find a set of N triplets $\{a'_k, \nu'_k, \phi'_k\}$ so that the reconstructed signal $f'(t)$, given by

$$f'(t) = \sum_{k=1}^{N} a'_k e^{i(\nu'_k t + \phi'_k)} , \tag{2}$$

is the best approximation to the original $f(t)$.

To find the triplets $\{a'_k, \nu'_k, \phi'_k\}$, we analyze the function $\psi(\nu)$ obtained as a scalar product of the original $f(t)$ and of the function $e^{i\nu t}$, weighted by the Hanning function $\chi(t) = 1 + \cos(\pi t/T)$:

$$\psi(\nu) = \frac{1}{2T} \int_{-T}^{T} f(t) e^{i\nu t} \chi(t) dt . \tag{3}$$

We look for the higher relative maxima ν'_j of $\psi(\nu)$ and set $a'_j = \psi(\nu'_j)$, and then we sort the N maxima for decreasing a'_j: $a'_1 \geq a'_2 \geq \ldots \geq a'_N$. We finally check if the original signal is well reconstructed by computing a χ^2 value. The accuracy of the algorithm is further tested by subtracting the largest components from $f(t)$ and reiterating the search for the basic

[1] Available at http://www.boulder.swri.edu/~hal/swift.html.

frequencies in the signal:

$$f(t) \longrightarrow f(t) - a_1' e^{i(\nu_1' t + \phi_1')} \ . \quad (4)$$

To estimate the precision of the frequency determination, we apply the FMA algorithm to the reconstructed signal to compute again the frequencies (Laskar et al. 1992). We find an error of the order of 10^{-10} yr^{-1} in the estimate of the proper frequency of Saturn Trojans.[2]

2.3. *Application of the FMA to the Sample of Saturn Trojans*

The basic frequencies that appear in the spectra of Trojan orbital elements are the libration of the critical argument $\lambda_T - \lambda_S$ and the circulation frequency g of the perihelion longitude $\tilde{\omega}_T$. The libration period of the critical argument is of the order of 800 yr, which is short compared to the circulation period of $\tilde{\omega}_T$, which is of the order of 2×10^4. We applied the FMA on the latter variable, which appears as a fundamental variable in secular theories. The critical argument, on the other hand, has a more complex behavior since its oscillation is not symmetric around the Lagrangian points. Its spectrum is characterized by a superposition of different frequencies.

In the FMA method we use the nonsingular variables h and k, defined as $h = e \cos \tilde{\omega}$ and $k = e \sin \tilde{\omega}$. For each orbit, we calculate the frequency and amplitude of the main components in the eccentricity, and we find three forced terms and the proper one. The frequencies of the three forced terms are determined by the fundamental frequencies g_5 and g_6, which are related to the revolution frequencies of the perihelion longitudes of Jupiter and Saturn, respectively. The largest forced component has the frequency g_6, while the second forced component has frequency g_5. The frequency of the third component is a linear combination of g_5 and g_6, namely, $2g_6 - g_5$. The proper component has frequency g and an amplitude equal to the proper eccentricity e_p (Milani 1993). In Figure 1 we show three examples of spectra of $f(t)$, where the proper component and the three forced ones are clearly visible. In the analysis we had to pay particular attention to separate the proper frequency g from the close frequency $2g_6 - g_5$. At low inclinations the proper frequency g is well separated from the nonlinear term $2g_6 - g_5$, but at high inclinations, however, when the orbits become unstable on a timescale shorter than 5 Myr, the two frequencies very often overlap.

With FMA the orbital stability is measured by the degree of diffusion of the proper frequency g with time. We have applied the FMA over a running window of $T_w = 4 \times 10^5$ yr over the 5 Myr of integration time span, every $T_s = 2 \times 10^5$ yr. These values were chosen after the analysis of a large number of cases. It was a good compromise between two opposite requirements: the need to keep the window large for a better definition of the spectral lines and, on the other hand, the necessity of keeping the window small in order to avoid the averaging out of the variations in the proper frequency g. If the window is too large, the risk is to underestimate the dispersion in g.

The proper eccentricity e_p for each virtual body is computed on the first window, while the proper libration amplitude D is derived as an average of the difference between the maximum and minimum value of the critical argument $\lambda_T - \lambda_S$ over 10 subwindows of 4×10^4 yr. The proper frequency g is computed on each running window, and the standard deviation σ_g of the g-values over the 5 Myr is derived as a measure for the diffusion rate of the orbit.

[2] The FMA software used in this paper is available at http://orsa.sourceforge.net.

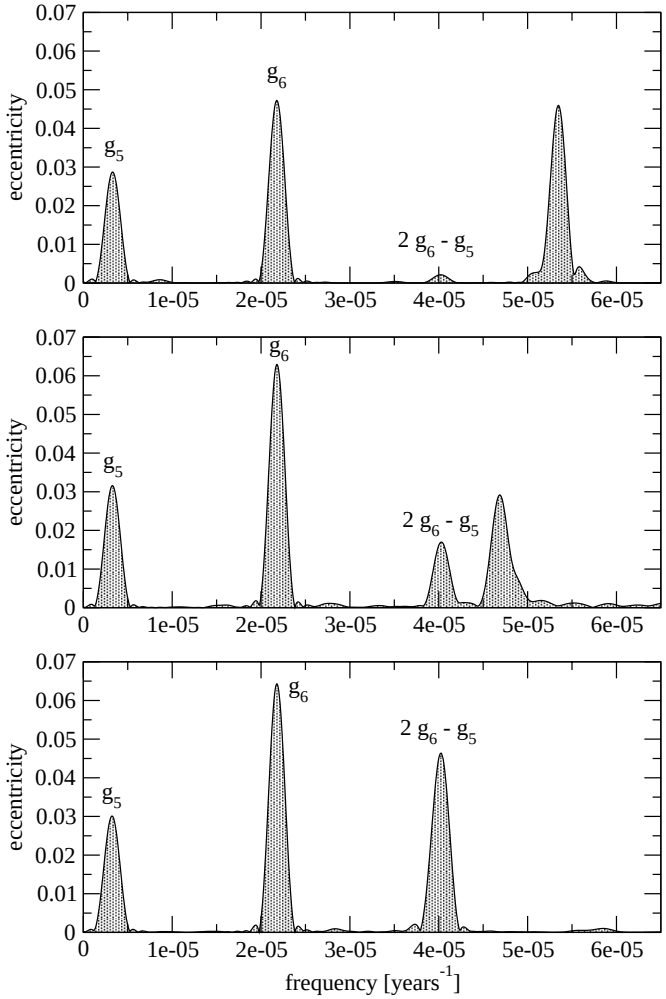

FIG. 1.—Spectra of three different virtual Saturn Trojans. The top panel has an inclination of 5°, the middle one of 10°, and the bottom of 20°. The peaks of the forced terms, in particular the one related to $2g_6 - g_5$, grow with inclination as g approaches these frequencies (see the classical linear theory for secular motion).

3. DIFFUSION PORTRAITS AT DIFFERENT INCLINATIONS

In Figure 2 we show the diffusion portraits in the space $e_p - D$ of the orbits of Saturn Trojans that survive at least over 5 Myr of numerical integration. Each diffusion portrait shows the stability of the proper frequency g for a fixed value of inclination ranging from 0° to 15°. All orbits with a starting inclination of 20° and larger became unstable within 1 Myr. The chaotic diffusion of g is measured as the logarithm of the relative change σ_g/g, where σ_g is the standard deviation of the frequency g computed over 25 windows (for those bodies surviving the whole integration). Different colors indicate a different diffusion speed: blue colors correspond to lower values of $-\log(\sigma_g/g)$ (we take the negative value of the logarithm to make the reading of the plots easier) and denote a fast diffusion and therefore

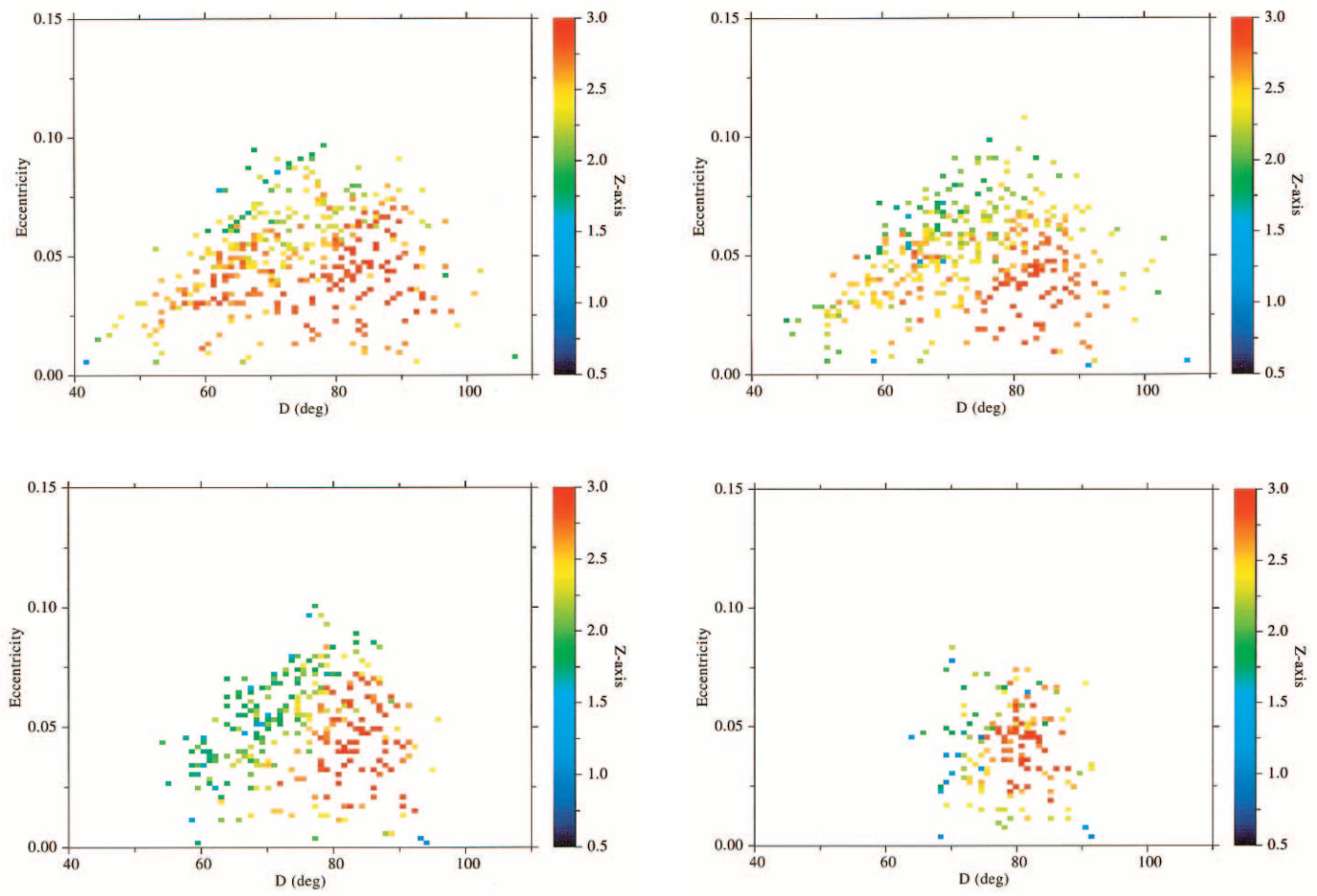

FIG. 2.—Diffusion portrait in the $e_p - D$ plane for Saturn Trojan orbits. The different color levels are defined by the negative value of the logarithm of the relative dispersion of the frequency $\epsilon = -\log(\sigma_g/g)$. The values range from 0.5 to 3 (blue to red). *Top left-hand panel*: inclination = 0°. *Top right-hand panel*: inclination = 5°. *Bottom left-hand panel*: inclination = 10°. *Bottom right-hand panel*: inclination = 15°.

chaos, while red colors related to values of $-\log(\sigma_g/g)$ of about 3 represent the more stable orbits. The value of 3 is the maximum we allow the color coding in order to better outline the stable regions. Only a few bodies have values up to 3.2 and are also coded red. For $i = 0°$, the red filled circles, corresponding to long-living Trojan orbits, are located at values of e_p around 0.05 and for $50° < D < 90°$. This stability area shrinks for increasing inclination, and it reduces to a smaller area centered at $D = 80°$. The stable region around $D = 60°$ visible at $i = 0°$ vanishes progressively at higher inclinations. For $i = 20°$, all the 1000 bodies of the sample become unstable within 1 Myr, while for $i = 30°$ and $i = 40°$, the escape timescale is so short (a few $\times 10^5$ yr) to prevent the application of the FMA. At high inclinations Saturn Trojan orbits seem to be strongly unstable. Low values of e_p imply that for most of the stable Trojans, the longitude of perihelion has a behavior called "paradoxical libration" (Beaugé & Roig 2001) because the proper eccentricity is smaller than that forced by Saturn. Indeed, the orbits found to be stable over timescales of the order of a few $\times 10^8$ up to 10^9 yr by de la Barre et al. (1996) and Melita & Brunini (2001) are in paradoxical libration. It is not clear whether this dynamical peculiarity is at the origin of stability, preventing, for example, the body to cross the mixed secular resonance $2g_6 - g_5$, or whether it is simply a consequence of dynamical stability at low proper eccentricities.

A question that can be addressed by the frequency analysis is the survival of a possible primordial population of Saturn Trojans: do the Trojan orbits with lower diffusion in the phase space survive over the solar system age? Following Melita & Brunini (2001), we can estimate the time span of stability from the dispersion σ_g/g with the following formula:

$$\log T = \log T_i - \log\left(\frac{\sigma_g}{g}\right), \tag{5}$$

where T_i is the length of the numerical integration, 5 Myr in our case, and T is the dynamical lifetime of the orbit. This formula implicitly assumes that the dispersion σ_g/g grows linearly with time. If we apply equation (6) to our results, we find that orbits with $-\log(\sigma_g/g) \geq 3$ are stable over the solar system age. Nesvorný & Ferraz-Mello (1997) gave a qualitative estimate of the diffusion time by modeling the evolution of the dispersion as a random walk process where the relative standard deviation σ_g/g is proportional to the square root of T_i. In this case even longer lifetimes can be deduced since over 5 Gyr and with $-\log(\sigma_g/g) \geq 3$ we would expect less than a 3% change in the frequency.

A more conservative approach consists in selecting some sample orbits within the stable regions, i.e., those with a lower diffusion speed in the frequency space (red filled circles in Fig. 2), and integrating them over the solar system

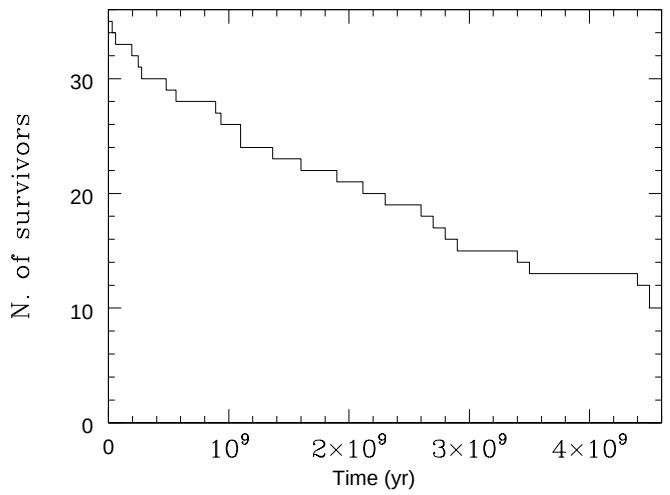

FIG. 3.—Survival curve for 35 Saturn Trojans picked up randomly within the "red" zone of stable orbits at 0° initial inclination.

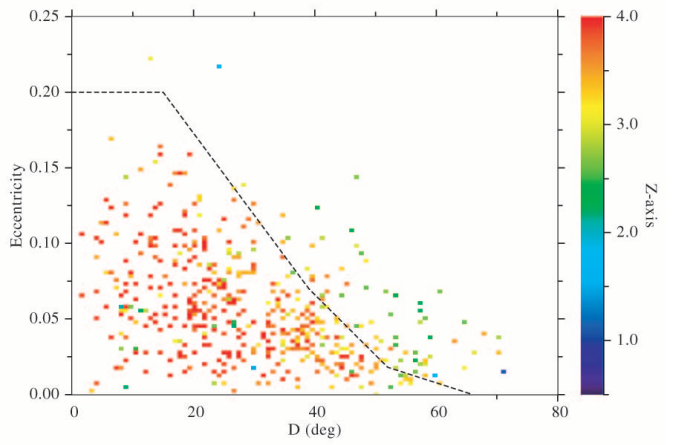

FIG. 4.—Diffusion portrait in the $e_p - D$ plane of real Jupiter Trojans. The range of values of the frequency dispersion $\epsilon = -\log(\sigma_g/g)$ is from 0.5 to 4 (blue to red). Red filled circles in this figure correspond to larger (one unity) ϵ values than in Fig. 2. The dashed line approximates the border of the Levison et al. (1997) stability region.

age. We chose 35 random orbits within the stability region with an initial inclination of 0°, proper eccentricity around 0.05, and libration amplitude around 80°. We integrated over 4.5 Gyr with a time step of 50 days. In Figure 3 we show the survival curve of the sample where at the end of the integration only 10 bodies survived. By fitting the data with an exponential decay curve, we obtain a half-life of 2.5×10^9 yr. A second sample of 35 objects selected among the yellow-green filled circles of Figure 2 has been integrated, and all the bodies become unstable within 100 Myr. If planetesimals were trapped as Saturn Trojans during the early stages of the solar system evolution, about 30% of those captured within the stable regions outlined in Figure 2 could still reside at present around the Lagrangian points of Saturn.

By comparing the results of the numerical integrations concerning the lifetime of Saturn Trojans and the analytical predictions by Melita & Brunini (2001) and Nesvorný & Ferraz-Mello (1997), it appears that both the formulas overestimate the real diffusion times, in particular that by Nesvorný & Ferraz-Mello (1997). A possible reason is that the diffusion rate of the proper frequency is not the same in different regions of the phase space and, as a consequence, it may not be appropriate to model the wandering of the proper frequency as a random walk with a fixed step size.

In order to test the reliability of the FMA method and to have an additional indication of the lifetime of Saturn Trojans, we computed diffusion portraits for the real Jupiter Trojans, most of which are believed to have survived over the age of the solar system, while some of them are on unstable orbits presumably due to past collisional events (Levison, Shoemaker, & Shoemaker 1997; Marzari et al. 1997). We integrated for 5 Myr the orbits of 495 numbered Trojans,[3] and we applied the FMA method using windows of 2×10^5 yr, half of the time span used to study the diffusion rate of Saturn Trojans. Values of $-\log(\sigma_g/g)$ up to 4.8 were obtained for some of the bodies, while the stability region defined by Levison et al. (1997) was retrieved by setting the minimum value of $-\log(\sigma_g/g)$ for stability equal to 4. In Figure 4 we show the diffusion portrait of Jupiter Trojans with the red filled circles now representing values of $-\log(\sigma_g/g)$ equal or larger than 4. As a reference we also plot the inner stability curve of Levison et al. (1997). By comparing Figure 2 to Figure 4, we notice that the stable area for Jupiter Trojans typically has values of $-\log(\sigma_g/g)$ one unit larger than that of Saturn Trojans. Translated in terms of lifetime via the two formulas reported above, this may mean that Jupiter Trojans can survive on average almost an order of magnitude longer in time. However, even this test does not give a definitive answer to the problem of survival time of Saturn Trojans. It only shows that "stable" Jupiter Trojans survive longer than "stable" Saturn Trojans. In any case, the stability area for Saturn Trojans is considerably smaller than that for Jupiter Trojans, and as a consequence, the number of expected Saturn Trojans should be significantly lower.

In Figure 4 there are a few blue-green filled circles and some yellow ones well within the stability region outlined by Levison et al. (1997) that seem to indicate less stable orbits. The blue filled circles at D lower than 40° are asteroids (29976) 1999 NE9, (24449) 2000 QL63, and (12929) 1999 TZ1, all on high inclination orbits ($i > 30°$). We integrated their trajectories over 4.5 Gyr, and they show large chaotic variations in the libration amplitude (almost a factor of 2), while eccentricity is constant on average. Asteroid (12929) TZ1 is ejected out of the Trojan swarm after 3.5 Gyr, while the remaining two bodies survive as Trojans until the end of the integration. Some of the yellow-green filled circles coincide with asteroids on chaotic orbits already studied by Milani (1993) via computation of the maximum Lyapunov exponent (see, for example, [1208] Troilus and [2146] Stentor). The possible sources of instability for these bodies are summarized in Milani (1993).

4. INSTABILITY AT HIGH INCLINATIONS: THE ROLE OF THE FORCING TERM $2g_6 - g_5$

The previous diffusion portraits show that the stability region for Saturn Trojans becomes smaller for increasing inclination until at $i \geq 20°$ all the orbits are unstable. A

[3] See http://www.lowell.edu/users/elgb.

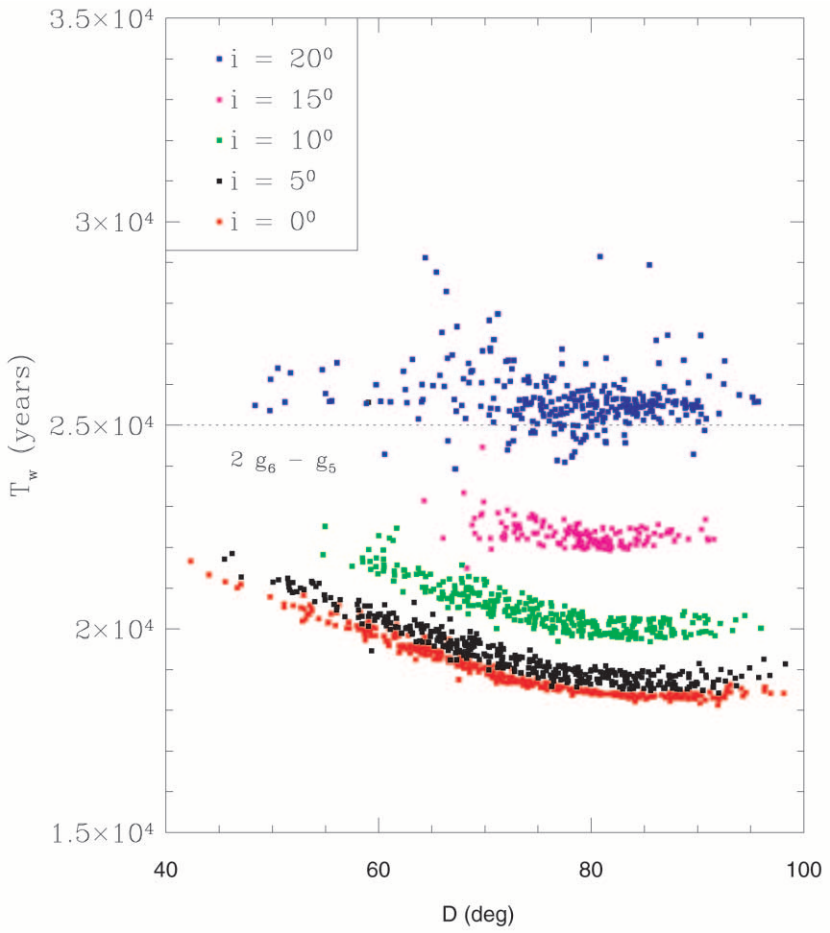

FIG. 5.—Period $T_{\tilde{\omega}}$, inverse of the proper frequency g, vs. libration amplitude D for different inclinations. For inclinations higher than 15°, the period of g approaches that of the forced term $2g_6 - g_5$ generating instability. All orbits with $i = 20°$ (*blue filled circles*) escape from the Trojan clouds within 1 Myr.

possible dynamical mechanism that destabilizes orbits at inclinations close to 20° is the vicinity of the proper frequency g to the forcing term $2g_6 - g_5$. As shown in Figure 1, g approaches $2g_6 - g_5$ with increasing inclination. This is further confirmed in Figure 5, where we plot the period of circulation of $\tilde{\omega}$ as a function of the libration amplitude D for different inclinations. For $i = 20°$, all the data are clustered around the period of the term $2g_6 - g_5$. Marzari & Scholl (2000) showed that a resonance between the proper frequency g and $2g_6 - g_5$ can indeed destabilize Saturn Trojan orbits by causing sudden jumps in the libration amplitude or eccentricity leading to close encounters with Saturn.

For inclinations larger than 20°, the dynamics appears to be more complex. By inspecting Figure 1 and by extrapolating equation (7) described in the next section, one should expect that the proper frequency g moves in between the $2g_6 - g_5$ and the g_6 frequencies at high inclinations. A resonance with g_6 may be at the origin of the fast instability we find for orbits at $i = 30°$ and $i = 40°$. Unfortunately, the orbits at large inclinations become unstable on a short timescale (a few $\times 10^5$ yr), and their behavior is highly irregular, preventing any reliable and meaningful analysis with the FMA method. Additional secular resonances involving the node of the Trojan orbit may also come into play when the inclinations are so high. For example, the nodal rate of the Trojan orbits with $i = 40°$ is close to the frequency $2g_5 - s_7$, and this may contribute to destabilize the orbit. Even the Jupiter's 2 : 5 resonance (Nesvorný & Dones 2002) can be a major reason.

5. A NUMERICAL THEORY FOR SATURN TROJAN MOTION

Using the outcome of the FMA theory, we can build up a semianalytical theory for the secular motion of Saturn Trojans in the variables h and k. According to Figure 1, the FMA method can be used to obtain for each Trojan orbit the values of the proper eccentricity and the forced components due to Saturn, $e_f^{\rm S}$, and Jupiter, $e_f^{\rm J}$. In Figure 6 we plot the values of $e_f^{\rm S}$ and $e_f^{\rm J}$ computed for all the Trojans, which are stable at least over 5 Myr, as a function of libration amplitude D. For both the forced terms, there is a clear dependence on D, while $e_f^{\rm S}$ is also related to the inclination of the Trojan orbit. From a least-square fit to the data plotted in Figure 6 with quadratic functions, we obtain the following approximate formulas for the two forced components of the Saturn Trojan eccentricity:

$$e_f^{\rm S} = \left(a_1^{\rm S} + b_1^{\rm S}\sin i\right) + \left(a_2^{\rm S} + b_2^{\rm S}\sin i\right)D + \left(a_3^{\rm S} + b_3^{\rm S}\sin i\right)D^2 ,$$
$$e_f^{\rm J} = a_1^{\rm J} + a_2^{\rm J}D + a_3^{\rm J}D^2 , \qquad (6)$$

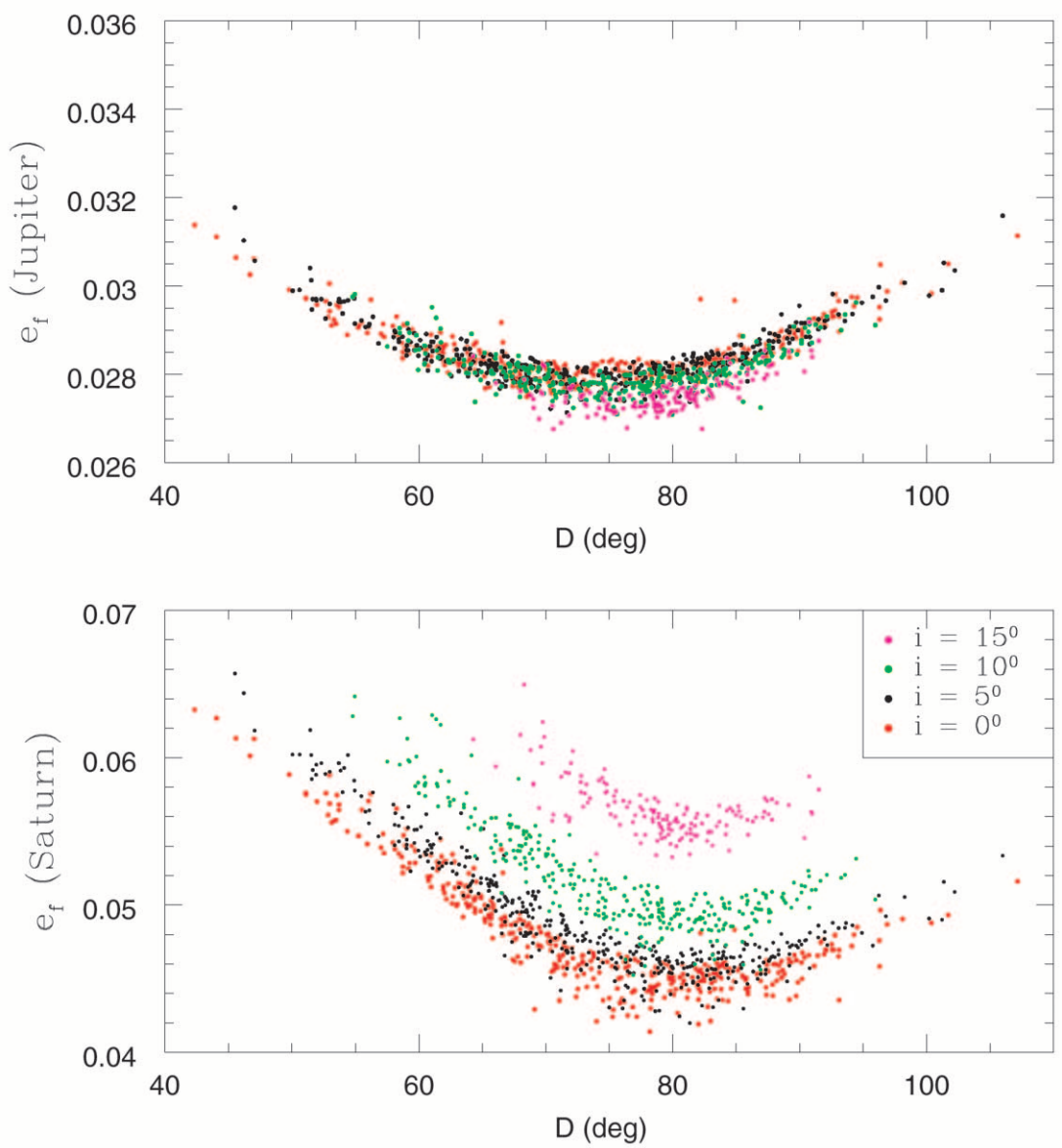

FIG. 6.—Values of the forced eccentricity by Saturn e_f^S and by Jupiter e_f^J as a function of the libration amplitude D and inclination i (different colors of the symbols). While for e_f^S a functional dependence on i is evident, for e_f^J, it is instead very weak.

where the numerical values of the constant coefficients are given in Table 1. The quadratic model adopted is robust, as confirmed by the goodness of the fit assessed with the χ^2 statistics. The weak diffusion around the quadratic behavior of the data is due to the choice of grouping the data at the beginning of the numerical integration according to the initial inclination that is not equal to the proper one but only close to it. The stronger scattering of some data is instead associated with the instability of the corresponding orbits. They survive over 5 Myr, but the amplitudes of the proper and forced eccentricities change rapidly over a timescale of 10^5 yr. They appear as blue filled circles in Figure 2.

The other relevant parameter for a secular theory of the h and k variables is the proper frequency g. From a least-square fit of the data in Figure 5 we obtain the following equation for g as a function of D and i:

$$g = (\alpha_1 + \beta_1 \sin i + \gamma_1 \sin i^2) + (\alpha_2 + \beta_2 \sin i + \gamma_2 \sin i^2) D + (\alpha_3 + \beta_3 \sin i + \gamma_3 \sin i^2) D^2 , \quad (7)$$

where g is given in yr^{-1} like the constants α_i, β_i, and γ_i (see Table 1 for the numerical values). For any Saturn Trojan, we can derive the h and k variables at any time from the following equations:

$$h = e_f^S \sin(g_6 t + \phi_S) + e_f^J \sin(g_5 t + \phi_J) + e_p \sin(g t + \phi) ,$$
$$k = e_f^S \cos(g_6 t + \phi_S) + e_f^J \cos(g_5 t + \phi_J) + e_p \cos(g t + \phi) , \quad (8)$$

where the phases are determined from the initial conditions.

TABLE 1

COEFFICIENTS OF THE SEMIEMPIRICAL MODEL FOR SATURN TROJAN ORBITS

Coefficient	Value
a_1^S	0.136138
a_2^S	−0.122716
a_3^S	0.040782
b_1^S	0.235529
b_2^S	−0.293451
b_3^S	0.110280
a_1^J	0.053075
a_2^J	−0.035824
a_3^J	0.013697
$\alpha_1(\mathrm{yr}^{-1})$	1.965599×10^{-5}
$\alpha_2(\mathrm{yr}^{-1})$	4.386980×10^{-5}
$\alpha_3(\mathrm{yr}^{-1})$	-1.374565×10^{-5}
$\beta_1\,(\mathrm{yr}^{-1})$	-3.012835×10^{-5}
$\beta_2\,(\mathrm{yr}^{-1})$	9.271595×10^{-7}
$\beta_3\,(\mathrm{yr}^{-1})$	1.188317×10^{-5}
$\gamma_1(\mathrm{yr}^{-1})$	6.197636×10^{-4}
$\gamma_2(\mathrm{yr}^{-1})$	8.191261×10^{-4}
$\gamma_3(\mathrm{yr}^{-1})$	2.108122×10^{-4}
$T_0\,(\mathrm{yr})$	738.350
$\rho_1(\mathrm{yr})$	−151.453
$\rho_2(\mathrm{yr})$	113.593

NOTE.—The independent variables are the libration amplitude D and the inclination i.

Also, the libration period of the critical argument $\lambda_T - \lambda_S$ depends on the libration amplitude D as shown in Figure 7. There is apparently only a weak dependence on i that we cannot resolve in the limited range of inclination where the Trojan orbits are stable. We decided, therefore, to neglect the dependence on i, and we fitted the data to a quadratic function in D:

$$T_l = T_0 + \rho_1 D + \rho_2 D^2 \ . \tag{9}$$

Equations (6)–(9) describe the main secular features of Saturn Trojan orbits and can be considered a good benchmark for analytical theories.

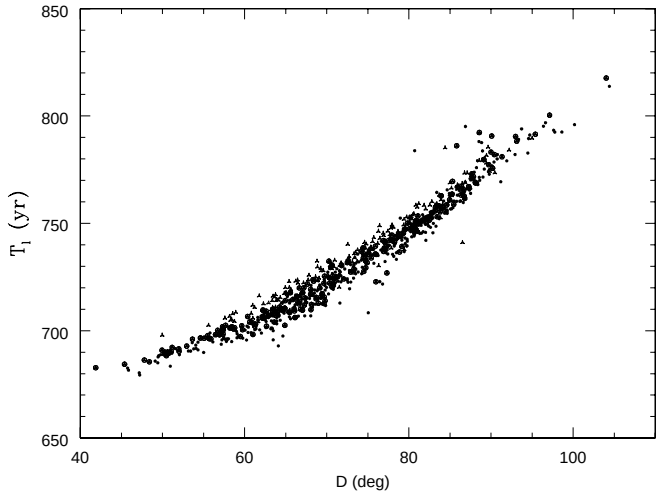

FIG. 7.—Period of libration of the critical argument $\lambda_T - \lambda_S$ as a function of the libration amplitude D for all inclinations, 0°–20°. Different symbols are for different inclinations.

6. CONCLUSIONS

By applying the frequency analysis method, we determined stability regions for virtual Saturn Trojans in the libration amplitude versus proper eccentricity space. We investigated the size of these regions as a function of inclination. We found stable orbits for low proper eccentricity and libration amplitudes around 80°. The majority of these orbits are in a state of "paradoxical" libration, a term proposed by Beaugé & Roig (2001). The stability region shrinks at higher inclination and totally disappears for $i > 15°$, probably because of secular resonances. With the FMA we find evidence that $2g_6 - g_5$ is responsible for instability at inclinations around 20°. This result is in good agreement with the work of Nesvorný & Dones (2002), who computed the maximum LCEs for inclined Saturn Trojans near L4.

We tested the reliability of the frequency analysis method by applying it to the known Jupiter Trojans. We retrieved the stability region outlined by the numerical integrations of Levison et al. (1997). The diffusion time of the fundamental frequencies of Jupiter Trojans appears to be an order of magnitude longer compared to Saturn Trojans.

The frequency analysis allows us to build a semianalytical secular model to the second order in the libration amplitude and the first order in inclination for the h and k variables. The libration period depends almost linearly on the libration amplitude.

What needs to be explored in more detail is the question of the lifetime of the stable orbits for the Saturn Trojans in our set. Can they survive over the solar system age? According to the formula given in Melita & Brunini (2001) and Nesvorný & Ferraz-Mello (1997), where the diffusion in the frequency space is modeled as a random walk, the answer is yes. However, our long-term integrations of sample orbits taken from the stable regions outlined in Figure 2 indicate a half-life of about 2.5 Gyr and invite then to more caution.

What are the sources for instability in the Saturn Trojan region? Nesvorný & Dones (2002) found large-scale chaos in Saturn's co-orbital space in the planar bicircular model, keeping both Jupiter and Saturn on circular orbits. Chaos is due to the overlap of Jupiter's 2 : 5 (Great Inequality) and Saturn's 1 : 1 mean motion resonances. Eccentricities of Trojan orbits are increased over timescales smaller than 10 Myr, and the Trojans are ejected after a close encounter with Saturn. In a comparable small region, eccentricities are not increased over the 10 Myr timescale. We (Marzari & Scholl 2000) found that in this 10 Myr stable region, the mixed secular resonance $2g_6 - g_5$ is a source for instability. Trojans may walk into this resonance on timescales longer than 10 Myr. The walk might be due to the overlapping of the 2 : 5 and 1 : 1 mean motion resonances. The efficiency of the mixed secular resonance to destabilize Trojan motion grows with increasing inclination according to our results. Additional sources of instability coming into play at high inclinations should be explored. Unfortunately, the lifetime of orbits with inclination larger than 20° is very short, preventing a detailed investigation of the dynamical mechanisms that destabilize these orbits.

We are grateful to the referee Luke Dones for his helpful comments.

REFERENCES

Beaugé, C., & Roig, F. 2001, Icarus, 153, 391
Carpino, M., Milani, A., & Nobili, A. M. 1987, A&A, 181, 182
de La Barre, C. M., Kaula, W. M., & Varadi, F. 1996, Icarus, 121, 88
Gomes, R. S. 1998, AJ, 116, 2590
Innanen, K. A., & Mikkola, S. 1989, AJ, 97, 900
Jewitt, D. C., Trujillo, C. A., & Luu J. X. 2000, AJ, 120, 1140
Laskar, J. 1993a, Physica, 67, 257
———. 1993b, Celest. Mech. Dyn. Astron., 56, 191
Laskar, J., Froeschlé, C., & Celletti, A. 1992, Physica, 56, 253
Levison, H., & Duncan, M. J. 1994, Icarus, 108, 18
Levison, H., Shoemaker, E. M., & Shoemaker, C. S. 1997, Nature, 385, 42
Marzari, F., Farinella, P., Davis, D. R., Scholl, H., & Campo Bagatin, A. 1997, Icarus, 125, 39
Marzari, F., & Scholl, H. 1998a, Icarus, 131, 41
———. 1998b, A&A, 339, 278
———. 2000, Icarus, 146, 232
Marzari, F., Scholl, H., Murray, C., & Lagerkvist, C. I. 2002, in Origin and Evolution of Trojan Asteroids, ed. W. Bottke, A. Cellino, P. Paolicchi, & R. Binzel (Tucson: Univ. Arizona Press), in press
Melita, M. D., & Brunini, A. 2001, MNRAS, 322, L17
Milani, A. 1993, Celest. Mech. Dyn. Astron., 57, 59
Nesvorný, D., & Dones, L. 2002, Icarus, in press
Nesvorný, D., & Ferraz-Mello, S. 1997, Icarus, 130, 247
Pollack, J., Hubickyj, O., Bodenheimer, P., Lissauer, J., Podolak, M., & Greenzweig, Y. 1996, Icarus, 124, 62
Wisdom, J., & Holman, M. 1991, AJ, 102, 1528